Journal of Korean Society of Remote Sensing, Vol. 4, No. 1, 1988

The Horizontal Wind and Vertical Motion Field Derived from the NOAA Polar Orbiting Satellites

Dong-Kyou Lee
Department of Atmospheric Sciences
Seoul National University
San 56-1, Shinrim-dong, Kwanak-Ku, Seoul 151, Korea
(Received January 2, 1988; Accepted March 15, 1988)

Abstract

The operational NOAA satellite temperature soundings are utilized to determine the horizontal wind and vertical motion fields for a polar low case over the East Asian region by solving the nonlinear balance equation and the omega equation. Preliminary results demonstrate that the balanced wind and vertical motion fields derived from the satellite data give reasonable synoptic patterns associated with the polar low. This encourages the use of satellite information as inputs in the numerical weather prediction models.

1. Introduction

The operational NOAA-series polar orbiting satellites now provide vertical temperature and moisture soundings. In recent years the vertical temperature and moisture soundings were derived from the TIROS-N series and their usefulness had been described by Hayden et al.(1981) and Smith et al.(1981). The high resolution temperature and moisture sounding data could be available at 06GMT and 18GMT and also in the data-void area over the ocean, such as the Yellow Sea and the East Sea. A major effort is needed to fully exploit the informations for improvement in weather forecasts.

One of the utilities of the satellite sounding data is the generation of wind field from the temperature field. To do this, geostrophic relation, gradient wind relationship and nonlinear balance equation have been used in serveral studies. Mills and Hayden(1983) derived winds from the geopotential fields using the gradient wind law and then these winds were used for the initialization of numerical simulations of a mesoscale model.

In this paper horizontal wind and vertical motion fields are to be determined from satellite temperature data by solving the nonlinear balance equation and the quasi-geostrophic omega equation respectively. The results are to be compared with the winds and vertical motions obtained from the radiosonde data.

2. Derivation of balanced wind and vertical motion

a. Balanced wind

The full non-linear balance equation for ψ in the cartesian coordinates with spherical terms neglected (Bengtsson and Temperton, 1979) is

$$\nabla^2\psi = -f \pm \left\{ f^2 + 2\nabla^2\phi - 2\frac{\partial f}{\partial y}\frac{\partial\psi}{\partial y} + \left(2\frac{\partial^2\psi}{\partial x\partial y}\right)^2 + \left(\frac{\partial^2\psi}{\partial x^2} - \frac{\partial^2\psi}{\partial y^2}\right)^2 \right\}^{1/2} \quad \cdots\cdots (1)$$

where ψ is the stream function of balanced wind, f is the Coriolis parameter, ϕ is the geopotential height and ∇^2 is $\frac{\partial^2}{\partial x^2} + \frac{\partial^2}{\partial y^2}$. The positive sign in Eq. (1) is taken in the Northern Hemisphere and negative in the Southern Hemisphere. For a real solution to exist, the geopotential height should satisfy the condition that the expression inside the square root is non-negative for the equation to be elliptic. A negative square root corresponds to non-elliptic case where $\nabla^2\phi$ is strongly negative, as in a high pressure area with strong anti-cyclonic curvature. A technique is to alter the geopotential height locally by constraining wind to have zero absolute vorticity, and thus Eq. (1) is elliptic everywhere.

For the quantity $\nabla^2\psi$ to converge over the domain, Eq. (1) may be solved by an iteration technique with prescribed ψ values at the boundary. Each iteration requires the solution of a Poisson equation for ψ with proper boundary conditions given by Bengtsson and Temperaton (1979). Then, the balanced winds are determined from ψ by the definition, $u = -\frac{\partial\psi}{\partial y}$ and $v = \frac{\partial\psi}{\partial x}$

b. Vertical motion

The quasi-geostrophic omega equation, a linear non-homogeneous differential equation of the second order for ω in the cartesian coordinates (Holton, 1979) is

$$\sigma\nabla^2\omega + f_0^2\frac{\partial^2\omega}{\partial p^2} = f_0\frac{\partial}{\partial p}\left\{J\left(\frac{\phi}{f_0}, \frac{1}{f_0}\nabla^2\phi + f\right)\right\} - \nabla^2\left\{J\left(\frac{\phi}{f_0}, \frac{1}{f_0}\frac{\partial\phi}{\partial p}\right)\right\} \cdots\cdots (2)$$

where ϕ is geopotential height, p is the pressure, $\omega(\equiv\frac{dp}{dt})$ is the vertical motion of the constant pressure surface, f_o is constant, σ is the stability parameter, and J is the Jacobian operator.

Eq. (2) may be solved by an iteration or a direct method of numerical solution of partial differential equation with the Dirichlet boundary condition. A simple coundition is used that $\omega = 0$ on all the boundaries, that is, zero at the upper and lower boundaries as well as at the lateral boundaries.

3. Satellite temperature data

Infrared radiance measurements were obtained from the NOAA-8 polar orbiting satellite for a polar low case on March 20, 1984 over the East Asia. Temperature and moisture profiles were retrieved from the radiance measurements using McIDAS III at the Cooperative Institute for Meteorological Satellite Studies at the University of Wisconsin in the U.S.A., The retrieved temperature data were analyzed approximately during the period from 2330GMT 19 March 1984 to 0040GMT 20 March 1984. Fig. 1 shows the tracks of subsatellite points and times of NOAA-8. The orbital path width of NOAA-8 at 40°N was 20° to 30° or less than 15° on either side of the subsatellite track. Thus, complete coverage for the East Asian region near 0000GMT 20 March was obtained by processing the two consecutive orbital passes (2230-2240 GMT. 19 March of NOAA-8 descending pass and 0030-0040 GMT 20 March of NOAA-8 descending pass).

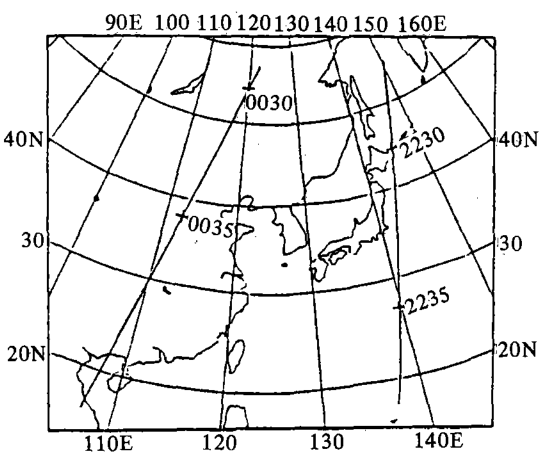

Fig. 1. Tracks of subsatellite point and times of NOAA-8 path for March 20, 1984.

The retrieval method used for the satellite temperature data of this study is the statistical regression retrieval algorithm developed at the University of Wisconsin(Smith *et al.*, 1981). This algorithm uses statistical relationships between satellite-measured radiances and atmospheric temperature profiles deduced from the analysis of large samples of previously observed radiances and collocated radiosonde reports. The number of retrieved temperature data for this study was about 850 in the region of 100°-144°E and 24°-60°N at 00GMT. The number of radiosonde stations were about 60 in the same region. Lee(1986) discussed the comparisions of the synoptic features between the satellite retrieved data and radiosonde data.

4. Results

The balanced winds and vertical motions on the standard pressure levels were obtained by solving Eqs. (1) and (2) numerically. Discussions on the results are made only for the 500mb level.

Fig. 2 shows the satellite derived balanced winds and observed radiosonde winds on the 500mb surface. General patterns of the two wind fields are well comparable to each other. Note that the positions of maximum u components roughly coincide each other. Magnitudes of the u component of the satellite balanced winds are as large as those of the observed winds except near the southern boundary, where the fixed boundary condition applied in solving the balance equation may cause reduced magnitude. Magnitudes of the v component of the satellite winds are approximately half smaller than those of the observed winds. However, the gradient of v component is corresponded to each other.

Fig. 3 shows vertical motion fields at the 500mb level computed from the both data sets. Rising motion area(negative ω values) obtained from the radiosonde data is well associated with the polar low while in the satellite data the rising motion areas are shifted to the east of the observed polar low and high resolution features are smoothed out although satellite data have more data points. It is noteworthy in Fig. 3 that magnitudes of the sinking motions obtained from both data sets are comparable each other.

The different results between the two data sets would be caused by cloud cover in the local areas, gap of radiance observation in the Yellow Sea and the East China Sea between the consecutive passes of the NOAA-8 satellite, and retrieval procedure in the satellite data.

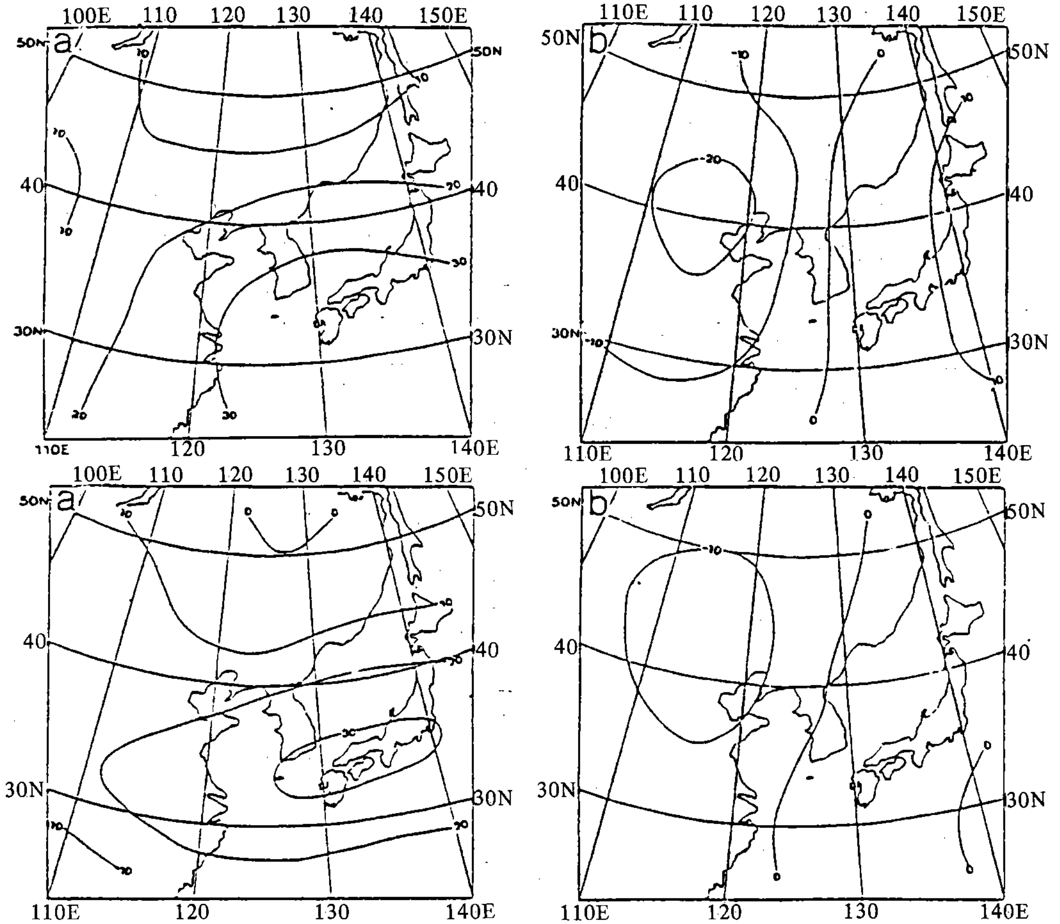

Fig. 2. 500mb radiosonde winds (upper panels) and satellite balanced winds(lower panels) for 00GMT 20 March 1984. Left panels(a's) are u component wind and right panels (b's) v component wind.

5. Conclusion

Wind and vertical motion fields were determined by solving the nonlinear balance equation and the omega equation using the vertical temperature soundings obtained from the polar orbiting NOAA satellite. Both the balanced winds and the vertical motion fields could identify the synoptic features associated with the polar low. Magnitude and general pattern in the balanced winds were well comparable to the observed winds. However, the vertical motion fields derived from the satellite data were shifted to the east of the corresponding fields obtained from the radiosonde data.

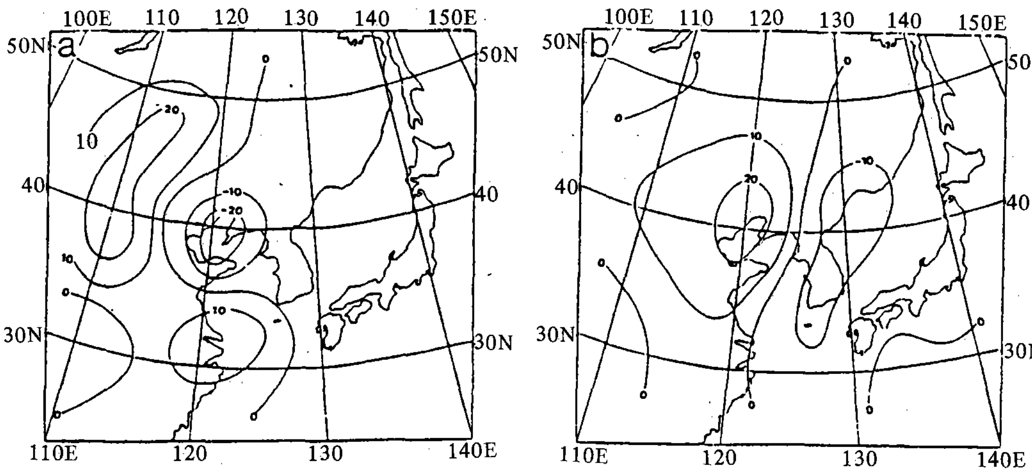

Fig. 3. 500mb vertical motion fields derived from the radiosonde data(a) and the satellite retrived data (b).

6. Acknowledgements

We are grateful to Dr. Bill L. Smith, Mr. Thomas Achtor and Mr. H. M. Woolf at the Cooperative Institute for Meteorological Satellite Studies, University of Wisconsin, U.S.A. for providing retrieved temperature data for this case study. This study was supported by the Korea Science and Engineering Foundation.

References

Bengtsson, L. and C. Temperton, 1979. Difference approximations to quasi-geostrophic models in *Numerical Methods Used in Atmospheric Models.* Vol. II. GARP Publications Series No. 17. World Meteorological Organization, p.499.

Hayden, C. M., W. L. Smith and H. M. Woolf, 1981. Determination of moisture from NOAA polar orbiting satellite sounding radiances. *J. Appl. Meteor.*, **20**, 450-466.

Holton, J. R., 1979. *An Introduction to Dynamic Meteorology.* Academic Press, p.391.

Kalb, M. W., 1985. Results from a limited area mesoscale numerical simulation for 10 April 1979. *Mon. Wea. Rev.*, **113**, 1644-1662

Lee, D. K., 1986. On the applicability of satellite temperature and moisture profiles for weather analysis in the East Asia. *J. Korean Meteor. Soc.*, **21**, 8-22.

Mills, G. A. and C. M. Hayden, 1983. The use of high horizontal resolution satellite temperature and moisture profiles to initialize a mesoscale numerical weather prediction model – A severe weather event case study. *J. Climate and Appl. Meteor.*, **22**, 649-663.

Smith, W. L., F. W. Nagle, C. M. Hayden and H. M. Woolf, 1981. Vertical mass and moisture structure from TIROS-N. *Bull. Amer. Meteor. Soc.*, **62**, 388-393.